SSRG International Journal of Mechanical Engineering
ISSN: 2348-8360/ https://doi.org/10.14445/23488360/IJME-V12I9P104

Volume 12 Issue 9, 37-45, September 2025

Original Article

Analyses of a Modified SCARA Manipulator (RRRRP) for Pick and Place Application

PVS Subhashini[1], Bharadwaj Aditya Singh[1]

[1]*Department of Mechanical Engineering, Vasavi College of Engineering, Hyderabad, India.*

[1]*Corresponding Author : pvs.subhashini@staff.vce.ac.in*

Received: 05 July 2025 Revised: 06 August 2025 Accepted: 07 September 2025 Published: 30 September 2025

Abstract *- Selective Compliance Assembly Robot Arm (SCARA) manipulator implementations are effective in the workplace (industrial) world, basically due to their exceptional accuracy and quickness in horizontal task assembly. The only constraint to their functionality is their modulus of vertical motion, which limits their applications with items in warehouse space and in very flexible manufacturing systems, with orientation being highly imperative, where vertical motion is an absolute movement aspect, it can be included. The study employed CAD modelling to engage design contextualization, draft a prototype, structural and kinematic contextualization, and motion contextualization, followed by material selection. This work also included kinematic modelling using the Denavit-Hartenberg method to conceptualize the capture of the workspace, trajectory planning, and finite element analysis of the theoretical concept for stress analysis under loading. A comparison to a traditional SCARA system model showed greater fit with diminished workspace and tolerating mass loads with a greater load capability factor, and it had reasonably significant trajectory planning accuracy. The stress calculations, once sent through the serial chain, confirmed that the system also remained confined to static equilibrium with insignificant displacements of stated loads and totally insignificant deflections that reside in elastic limits. Overall, the ability to realize additional functionality with the proposed product is beneficial both in the workplace by having a greater ability to provide a broader functionality workspace with items that require movement in both planes.*

Keywords *- Modified SCARA, CAD modelling, Motion study, Mathematical modelling, 5 DOF, Pick and place operations.*

1. Introduction

SCARA manipulators are well known for their application in assembly operations because they have high speed of operation, accuracy, and reliability. SCARA manipulators are especially suited for assembly, packaging of components, and the manufacture of electronic devices. The structural design of a SCARA manipulator includes a significant strength - allowing for flexibility in the X–Y plane, while displaying rigidity in the Z-axis. Because of this, SCARA manipulators are very well suited to high-precision operations in horizontal planes. There is thus a need for manipulators to work in the horizontal and vertical planes to achieve flexibility in orientations.

This clearly signals a gap in both research and practical application. Therefore, the aim is to develop the traditional SCARA architecture by modifying the action in such a manner that the motion capabilities are extended and thus greatly exploit the benefits of speed, accuracy, and lower costs are still available. Any augmentations would greatly increase and expand the functioning of SCARA manipulators, making them user-friendly and easier to manoeuvre for multiple industrial applications.

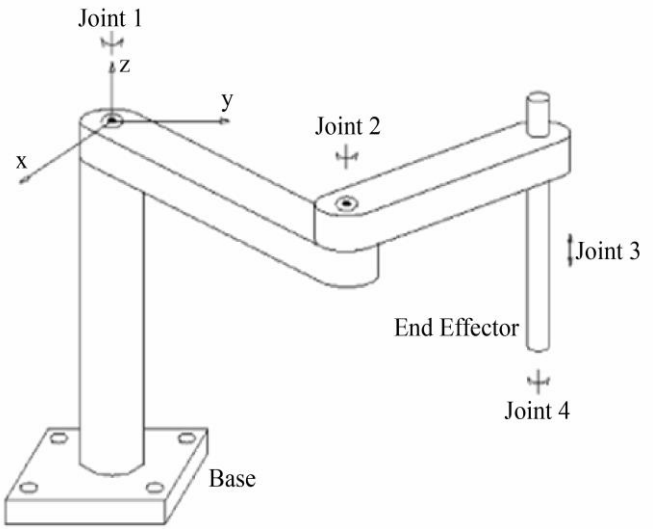

Fig. 1 Configuration of traditional SCARA

This study presents an improved SCARA manipulator with five degrees of freedom, with four revolute joints and one prismatic joint. Unlike traditional SCARA architectures, the

improved design facilitates smooth functional use in both horizontal and vertical planes - thus extending its flexibility and use for a broader range of industrial automation applications.

This study provided a comparative assessment of the new 5-degree-of-freedom SCARA manipulator versus traditional frameworks. The results show that the reinterpretation represents a dramatic change as opposed to an incremental change. This more sophisticated manipulator showed increased flexibility, improved structural integrity and more engagement for transitional or operational manipulation applications, which makes for an efficient solution for a wide range of manufacturing and automation applications.

SCARA Robots were born from the industrial demand for precision and efficiency in small production lots. Early on, Yamazaki [1] described the challenges he first faced when assembling wristwatches, which Dr. Hiroshi Makino's team addressed with a new degree of selective compliance in the X-Y plane to create a robot that achieved cost, labour and delivery time savings that established SCARA robots as credible devices for dedicated assembly projects.

Low-cost, without loss in performance, has always been a priority. Shariatee et al. [2] presented the FUM SCARA robot, made only from commercial, off-the-shelf components and was able to achieve ±0.01mm repeatability and high speeds. Conducting finite element analysis and utilising adaptive control architectures utilization increased its industrial application and research applicability.

Recent literature focuses on SCARA's responsiveness to a dynamic production landscape. Suri et al. [3] studied the Delta SCARA robot and underscored adapting and integrating other surrounding devices within modular production lines. This study found SCARA robots offered better workflow efficiency compared to Cartesian systems and represented a new level of versatility in solving contemporary automation issues.

Control systems have made gains as well, although the first wave of SCARA robots had only limited intelligence. Mohammed et al. [4] used ANFIS-based controllers for optimization the trajectory, while Tay et al. [5] emphasized the need to select an appropriate controller for the application within an Industry 4.0 architecture. AI and IoT's growing integration with SCARA robots is continuously extending their landscapes of possibility, including some robots with remotely operated and high-tech intelligent decisions.

The thrust area of research is mostly centred on adaptive control and overcoming nonlinear control. Garg's [6] studies represent early work on handling parametric uncertainty. Lee et al. [7] extended this work into sliding mode control to achieve robustness against disturbance.

Most recently, Bouzid et al. [8] and Panchanand Jha et al. [9] applied neural net learning to address their kinematics problems with the goals of reduced computation time and less reliance upon 'off the shelf' models.

The recent methods include Mittal RK et al. [10], who presented reinforcement learning for path planning, Tay, See Han et al. [11], who proposed adaptive algorithms for payload variation, and Ning, W et al. [12], who have applied topology optimization with the goal of reducing weight.

Liu et al. [13] have enabled a standard set of studies on workspace dynamics, while Qiu et al. [14] studied complex inverse kinematics, and Chen et al. [15] studied dynamic error compensation, which were able to further enhance SCARA system performance. Finally, Khan et al. [16] and Mohammed, Yousif et al. [4] implemented vision systems and fuzzy logic to increase systems' adaptability to uncertain work environments.

From the literature, SCARA robots were developed to face industrial automation challenges, especially in precision assembly. It is clear that in order to maximize the benefits of SCARA and overcome the workspace limitation, a modified SCARA with 5DOF is proposed.

2. Methodology

The SCARA manipulator was redesigned in multiple phases, beginning with the 3D models in SolidWorks. Each link and joint was modeled as a separate part and later assembled into the final manipulator. The focus was on integrating four revolute joints with a single prismatic joint to attain rigidity while providing the needed vertical flexibility.

After the CAD model was completed, a structural analysis was carried out to confirm the response to load. The analysis showed areas of stress concentration and confirmed that the manipulator will accept loads expected while causing minimal deflection.

The next step involves a kinematic study using a Denavit–Hartenberg (DH) convention to determine the forward kinematic equations. The DH convention provided a standardized way to determine realizable workspace limits and the end-effector trajectories. The output of this step will be used to tune the joint parameters and modify the dexterity of the manipulator.

To test real-world performance, we carried out motion simulations using SolidWorks Motion and MATLAB. These simulations created normal pick-and-place cycles while testing the manipulator's ability to use both a horizontal and vertical orientation. The tests also evaluated the smoothness and stability against various payloads.

Recorded the results from each testing stage in graphs, tables, and images. In totality, these results provided a good indication of how the design would perform in practice.

2.1. Modelling

The simulation of the modified SCARA manipulator begins by modeling it in three dimensions in a CAD environment. First, the individual links were modeled in the SolidWorks Part environment and then assembled in the Assembly Environment to produce the full manipulator assembly. Then the CAD Motion tool was used to define the types of motion between joints, and to study how the system behaved dynamically. At this point, detailed studies may have been done to show how the manipulator was able to perform.

One important part of the design was the Base, as shown in Figure 2. The Base provided structural support to the manipulator and was the primary attachment point for Link 1 and other parts of the system. The Base was designed to ensure that the manipulator was rigid, stable and aligned accurately. In the next section are the specifications of the Base.

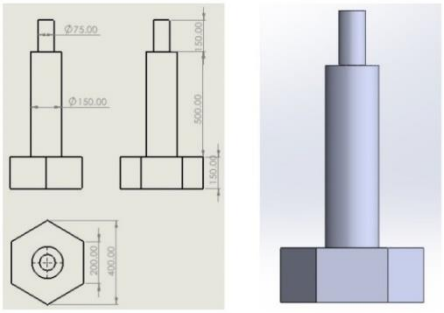

Fig. 2 Base

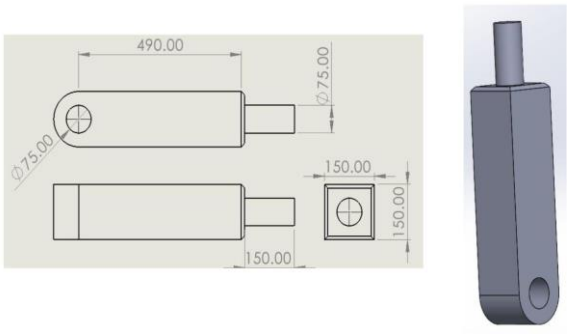

Fig. 3 Link 1

The second component is Link 1, shown in Figure 3, and it allows the manipulator flexibility in the horizontal plane. It is modeled and designed as per the following dimensions. Figure 4 shows component Link 2, which gives the manipulator flexibility in the vertical plane. It is modeled and designed as per the following dimensions. Figure 5 shows Link 3, which gives flexibility to the drill bit so that it can change the drilling angle. It is modeled and designed as per the following dimensions.

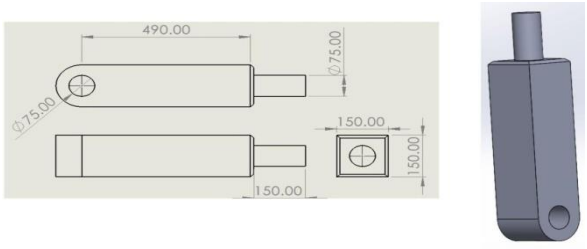

Fig. 4 Link 2

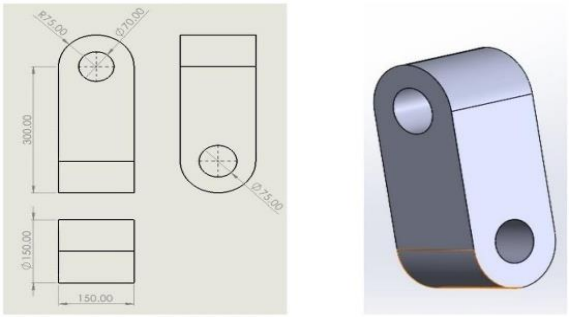

Fig. 5 Link 3

In Figure 6, the component shown is Link 4, which allows the drill bit flexibility, applied to end-effector adjustment. It is modeled and designed based on the following dimensions.

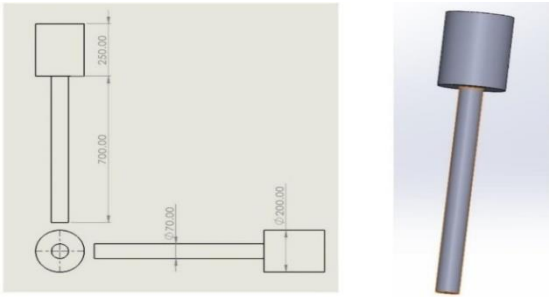

Fig. 6 Link 4

The next component shown in Figure 7 is the end-effector. The end-effector has two gripping links to hold the object, which performs the pick and place operation, as shown in the figure and dimensions in the table below: The end-effector has a subassembly which has a gripper hub, gripper finger, gripper link and gripper rotor link, whose dimensions are shown below:

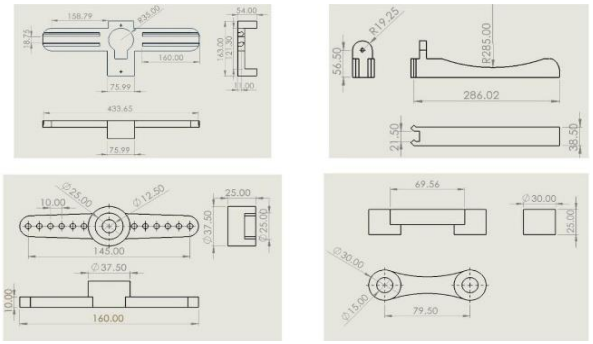

Fig. 7 End-effector parts diagram

The end-effector assembly of the gripper is shown in Figure 8, which defines the relationship between the components. The goal of the gripper is to hold and stabilize the object. The end-effector, which connects to the gripper, is therefore a subassembly of the end-effector.

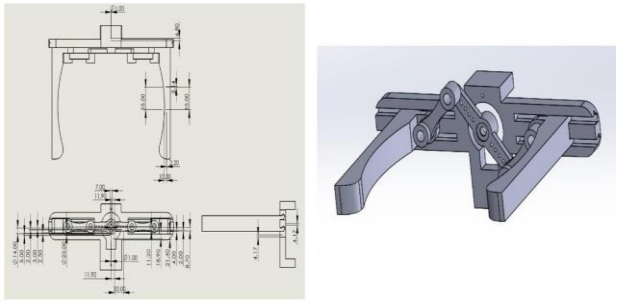

Fig. 8 End-effector Assembly

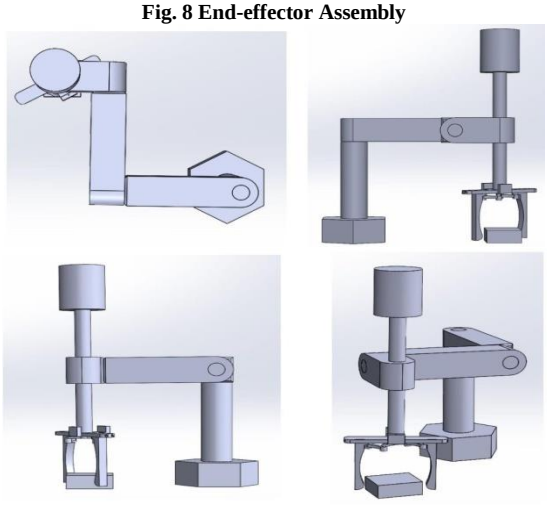

Fig. 9 Assembly of the manipulator in different views

The manipulator's assembly uses an assembly environment in CAD software. The parts are connected to each other, and to assume different assembly mates includes different types, as seen in Figure 9.

The work environment of the manipulator has an object that has to be picked and placed in the rack. The environment of the manipulator is shown in Figures 10, and 11.

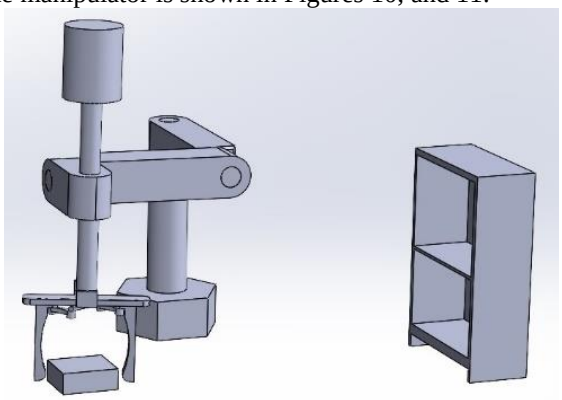

Fig. 10 Modified SCARA manipulator with work part

3. Mathematical Modelling

The forward kinematics of the altered SCARA manipulator is defined according to the Denavit–Hartenberg (DH) convention. This convention allows for the specification of homogeneous transformation matrices for each joint, leading to known end-effector position and orientation.

In order to preserve consistency in spatial depiction, coordinate frames are systematically assigned according to the axis of rotation for each joint. The kinematic structure of the manipulator is then defined completely in terms of the DH parameters.

Were,
link length, a = distance from zi to zi+1 measured along xi
Link twist, α = angle from zi to zi+1 measured about xi
Joint distance d distance from xi-1 to xi measured along zi
Joint rotation ɵ= angle from xi-1 to xi measured about zi

The simulations indicated that the proposed model achieved broad workspace coverage and preserved accurate trajectories during operation, both of which are necessary for reliable manipulator operation.

With respect to the DH parameters, the link length is decidedly the paramount parameter as it is most directly related to the reach of the manipulator and overall configuration of the workspace.

The Kinematic equations of the manipulator are given by the DH Matrices.

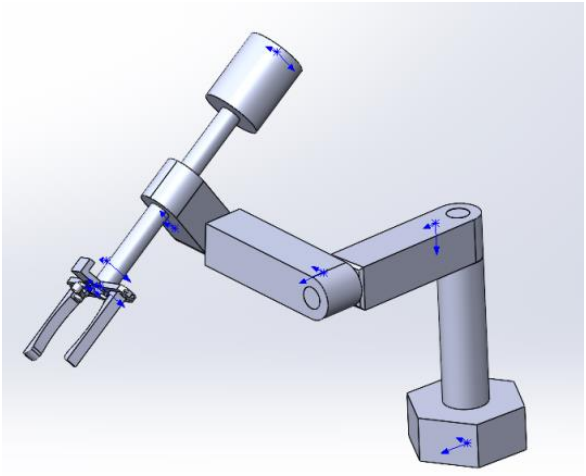

Fig. 11 Modified SCARA in another view

The link transformation matrix is given by:

$$ {}^{i-1}T_i = \begin{bmatrix} cos\theta_i & -sin\theta_i cos\alpha_i & sin\theta_i sin\alpha_i & a_i cos\theta_i \\ sin\theta_i & cos\theta_i cos\alpha_i & -cos\theta_i sin\alpha_i & a_i sin\theta_i \\ 0 & sin\alpha_i & cos\alpha_i & d_i \\ 0 & 0 & 0 & 1 \end{bmatrix} \quad \ldots(1) $$

Table 1. DH parameters of modified SCARA manipulator

link(i)	a	α (degrees)	d	ɵ
base (0)	0	-90	d_1	$ɵ_1$
1	0	-90	d_2	$ɵ_2$
2	0	90	0	$ɵ_3$
3	l_3	0	0	$ɵ_4$
4	0	0	d_5	0

The transformation matrices obtained for each link are as follows

$$ {}^{0}T_1 = \begin{bmatrix} c_1 & 0 & -s_1 & 0 \\ s_1 & 0 & c_1 & 0 \\ 0 & -1 & 0 & 0 \\ 0 & 0 & 0 & 1 \end{bmatrix} \quad (2) $$

$$ {}^{1}T_2 = \begin{bmatrix} c_2 & 0 & s_2 & 0 \\ s_2 & 0 & c_2 & 0 \\ 0 & -1 & 0 & 0 \\ 0 & 0 & 0 & 1 \end{bmatrix} \quad (3) $$

$$ {}^{2}T_3 = \begin{bmatrix} c_3 & 0 & s_3 & l_3 * c_3 \\ s_3 & 0 & -c_3 & l_3 * c_3 \\ 0 & 1 & 0 & 0 \\ 0 & 0 & 0 & 1 \end{bmatrix} \quad (4) $$

$$ {}^{3}T_4 = \begin{bmatrix} c_4 & -s_4 & 0 & 0 \\ s_3 & c_4 & 0 & 0 \\ 0 & 0 & 1 & 0 \\ 0 & 0 & 0 & 1 \end{bmatrix} \quad (5) $$

$$ {}^{4}T_5 = \begin{bmatrix} c_5 & -s_5 & 0 & 0 \\ s_5 & c_4 & 0 & 0 \\ 0 & 0 & 1 & d_5 \\ 0 & 0 & 0 & 1 \end{bmatrix} \quad (6) $$

The final transformation for the manipulator is obtained by multiplying (2), (3), (4), (5) and (6).

$$ {}^{0}T_5 = {}^{0}T_1 {}^{1}T_2 {}^{2}T_3 {}^{3}T_4 {}^{4}T_5 $$

$$ {}^{0}T_5 = \begin{bmatrix} (s_1s_3 + c_1c_2c_3)c_4 - s_2s_4c_1 & -(s_1s_3 + c_1c_2c_3)s_4 - s_2c_1c_4 & -s_1c_3 + s_3c_1c_2 & -d_5(-s_1c_3 + s_3c_1c_2) + l_3(s_1s_3 + c_1c_2c_3) \\ (s_1c_2c_3 - s_3c_1)c_4 - s_1s_2s_4 & -(s_1c_2c_3 - s_3c_1)s_4 - s_1s_2c_4 & s_1s_3c_2 + c_1c_3 & d_5(s_1s_3c_2 + c_1c_3) + l_3(s_1c_2c_3 - s_3c_1) \\ -s_2c_3c_4 - s_4c_2 & s_2s_4c_3 - c_2c_4 & -s_2s_3 & -(d_5s_3 + l_3c_3)s_2 \\ 0 & 0 & 0 & 1 \end{bmatrix} \quad (7) $$

4. Structural Analysis

With SCARA manipulators, rigid body analysis is performed using CAD-based simulation packages, generally in the context of transient structural analysis or using the rigid dynamics module. The manipulator model will depend on the configuration of the SCARA, but once the model is generated, its motion and load characteristics can be assessed accurately. This is an important piece of analysis because it can give useful output on parameters like resultant displacement and system responses with changing conditions.

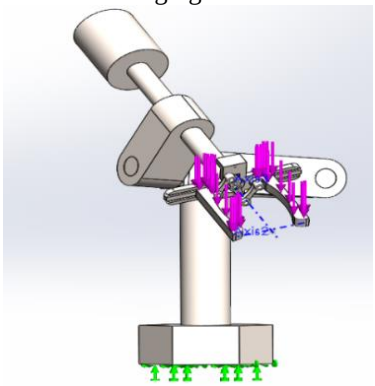

Fig. 12 Force application on the assembly of the modified SCARA

The Base of the manipulator remains stationary to analyze the stress and resultant displacement of the manipulator with a load of 100N acting on the end-effector, which is shown in Figures 12, 13, and 14.

In a nutshell, rigid body dynamics is the study of bodies that do not deform from their shape. Rigid body dynamics focuses on the motion of particles in a body that maintain a fixed relative distance. While a rigid body is subject to external forces or during the actuation of the end-effector body, each manipulator link is modelled as a rigid body with the Base as a fixed body, allowing it to be stable. This analysis was intended to simplify the yaw angle and configuration analysis while still being reasonable in how it looked to function in the real world.

The analysis was for the rigid body of the manipulator under applied loads of 100N. The final evaluation for the maximum stress was 1.81e+07 N/m2, and the final evaluation for the resulting displacement was 0.24 mm.

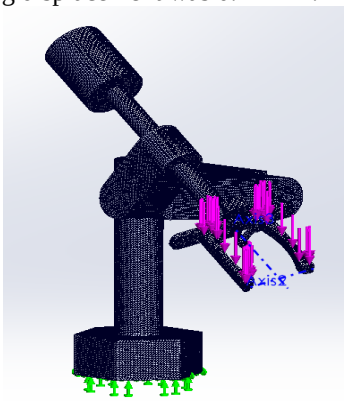

Fig. 13 Fine mesh generation of the manipulator in CAD

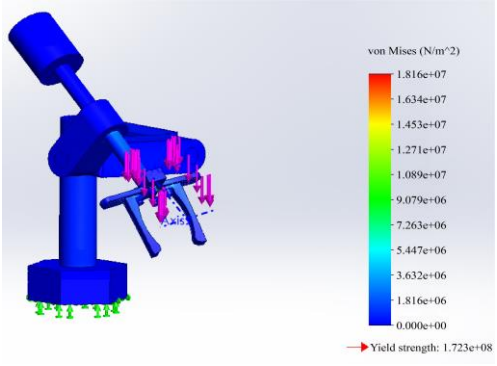

Fig. 14 Stress analysis

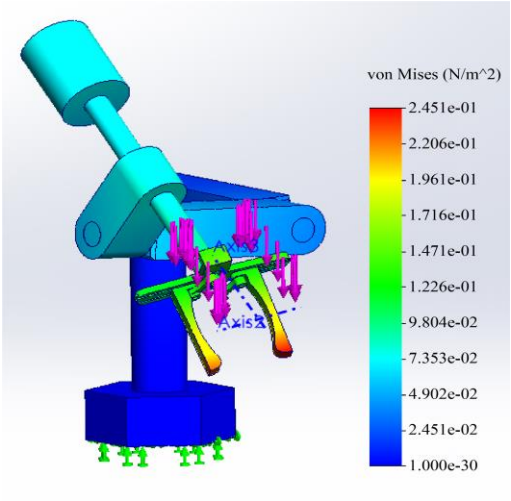

Fig. 15 Resultant displacement

5. Motion Analysis

The manipulator is oriented in the initial position, as shown in Figure 16. Each joint of the manipulator uses a motor simulated through CAD to make the movements of the manipulator. The angular displacement is input for the first three rotational joints. For the fourth rotational joint, angular velocity is input, and for the prismatic joint, linear displacement is input.

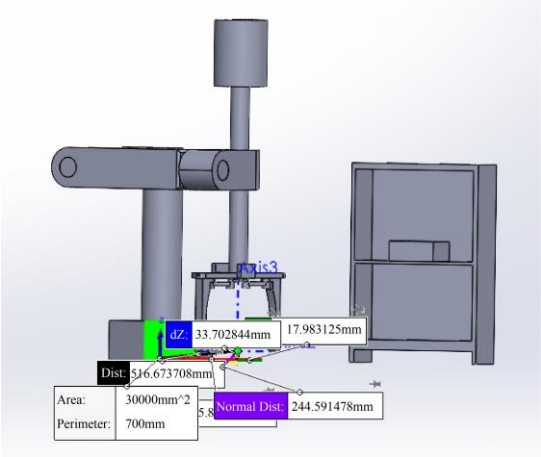

Fig. 16 Pick up point in horizontal plane

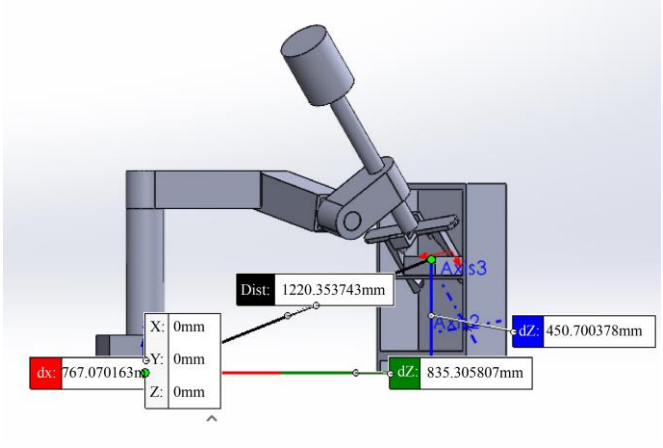

Fig. 17 Placing position in the vertical plane

Figures 17 and 18 demonstrate the manipulator modelling in SolidWorks 2023 and the end effector coordinates, respectively. The kinematic analysis is done in SolidWorks; the end-effector trajectory is illustrated in Figure 18.

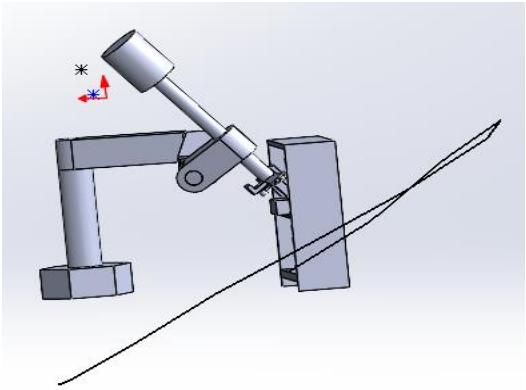

Fig. 18 Path of the end effector

6. Results

6.1. Angular Displacement, Angular Velocity and Angular Acceleration Plots of Each Joint for the Path

6.1.1. Joint 1

The first revolute joint demonstrated smooth angular kinematics, with consistent displacement propagation in a uniform manner based on what motion was applied to the input during the simulation cycle (Figure 19). The angular velocity and acceleration plots showed the same thing for input motion (Figures 20 and 21) while the linear velocity trajectory (Figure 22) seemed to show few drastic performance spikes.

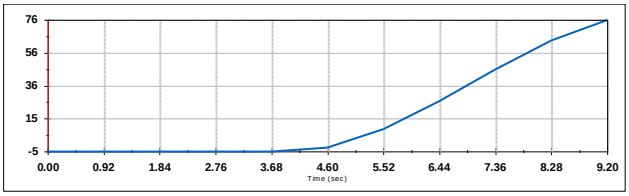

Fig. 19 Angular displacement of joint-1

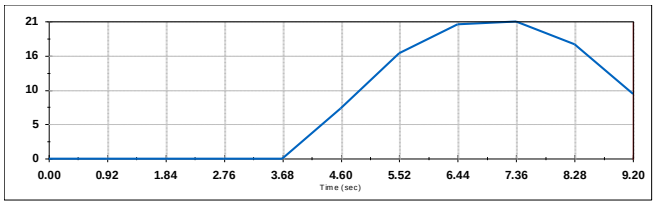

Fig. 20 Angular velocity of joint-1

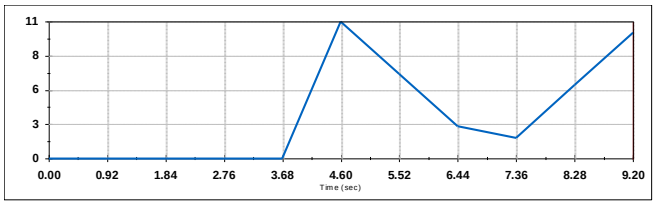

Fig. 21 Angular acceleration of joint-1

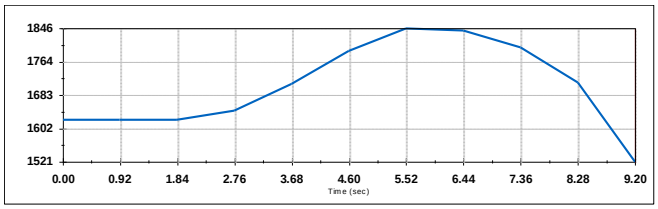

Fig. 22 Linear velocity of joint-1

6.1.2. Joint 2

Figures 23-26 showed that joint 2 underwent a negative angular displacement, which shows a counter-rotation of joint 1. The gentle slope of the velocity and acceleration curves also demonstrates the joint motion control that was acting on joint 2, and there is still some level of accuracy that can be attained with multi-axial coordination.

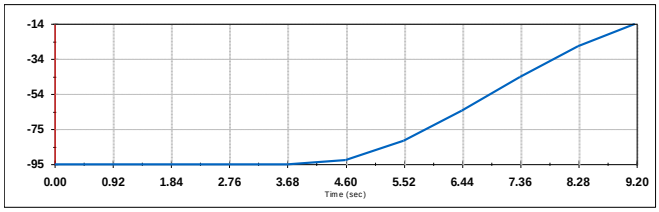

Fig. 23 Angular displacement of joint-2

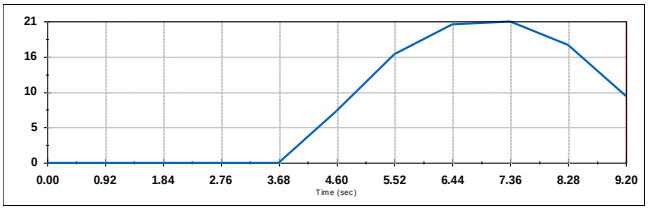

Fig. 24 Angular velocity of joint-2

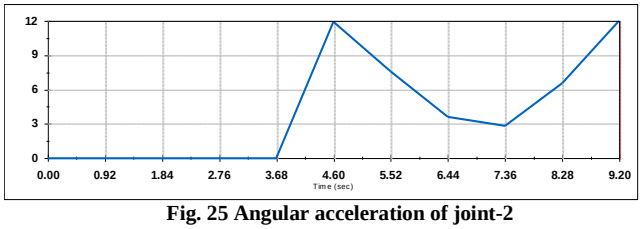

Fig. 25 Angular acceleration of joint-2

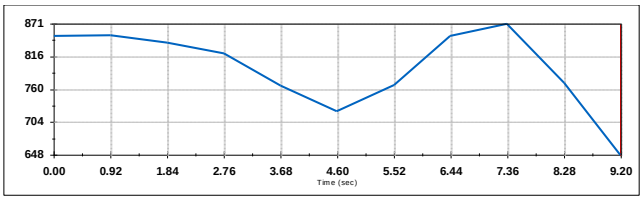

Fig. 26 Linear velocity of joint-2

6.1.3. Joint 3

Figures 27–29 illustrate the motion response of joint 3. Compared to the earlier joints, the acceleration shifted more noticeably, which implies that careful tuning of this joint is significant for smooth trajectories.

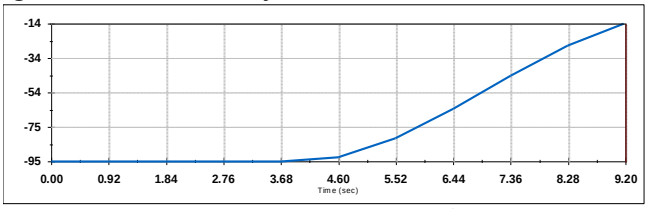

Fig. 27 Angular displacement of joint-3

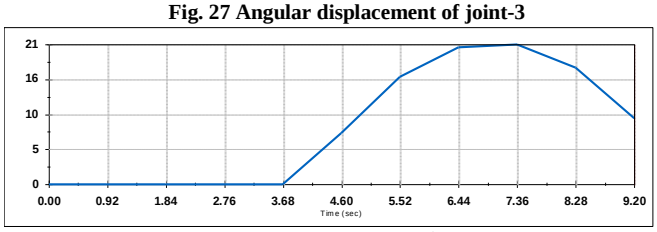

Fig. 28 Angular velocity of joint-3

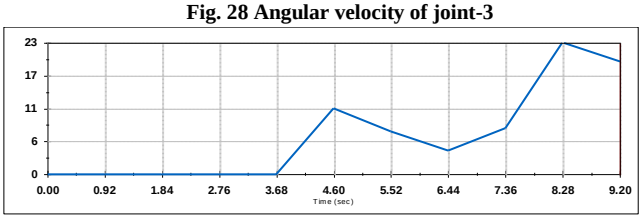

Fig. 29 Angular acceleration of joint-3

6.1.4. Joint 4

The final revolute joint (Figures 30–33) had a greater angle of motion and greater velocity changes, as might be expected for joints toward the end of the manipulator. The motion was still stable during the tests, and no inconsistencies were observed after a number of repetitions.

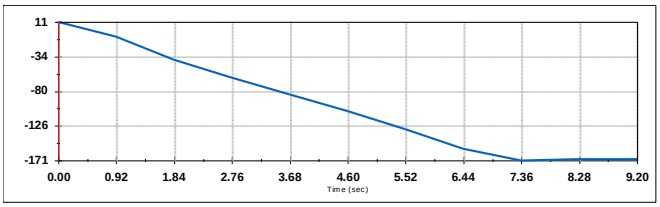

Fig. 30 Angular displacement of joint-4

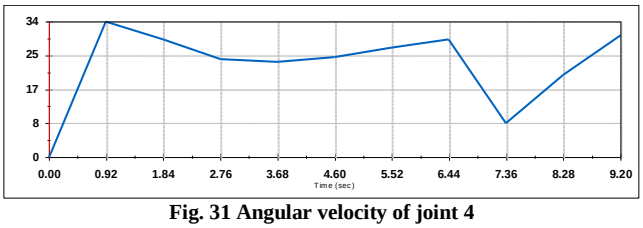

Fig. 31 Angular velocity of joint 4

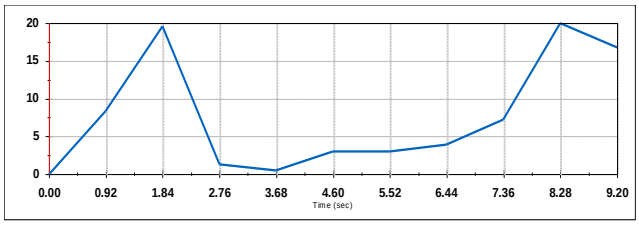

Fig. 32 Angular acceleration of joint-4

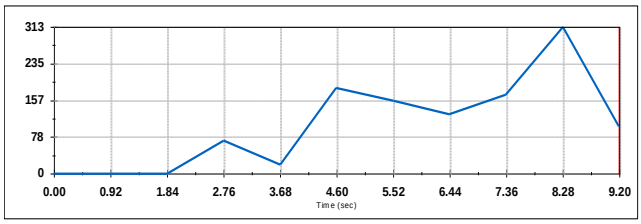

Fig. 33 Linear velocity of joint-4

6.2. Roll, Pitch and Yaw Plots of Each Joint for the Path

The Roll, Pitch, and Yaw plots of every joint are the plots of the orientation of a robotic joint in the form of its rotational motion around each axis. In order to analyze how every joint accounts for the joint motion of the robot, the roll, pitch and yaw plots of the manipulator were examined and displayed in figures 34, 35, 36, respectively.

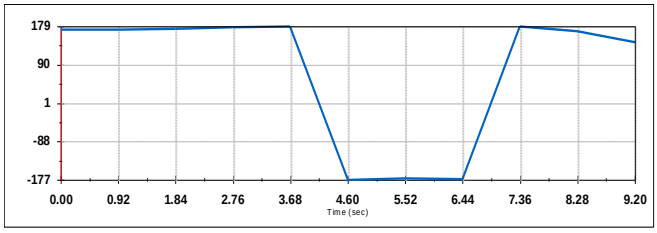

Fig. 34 Roll Vs Time

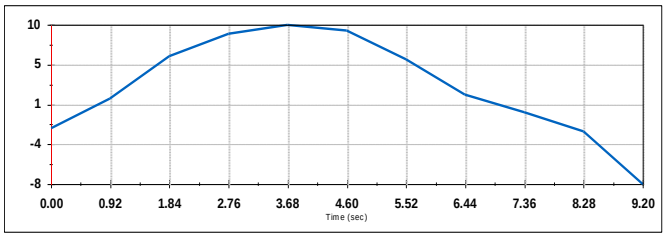

Fig. 35 Pitch Vs Time

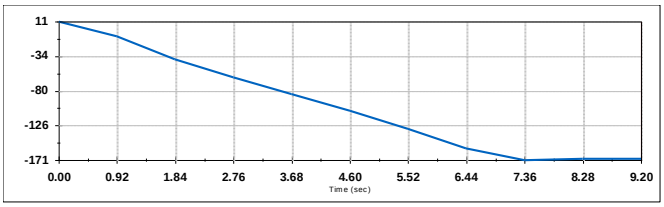

Fig. 36 Yaw Vs Time

7. Conclusion

This paper introduces an innovative 5-DOF SCARA manipulator developed to increase efficiencies in pick-and-place operations in both vertical and horizontal positions. The system was modeled using CAD, motion analyses and a detailed study of the kinematics.

The Denavit–Hartenberg (DH) convention was used to develop the forward kinematic equations used in the kinematics study. Structural testing was completed at a load of 100 N. The manipulator remained steady under load and showed it would be able to withstand stresses without failure. The experienced stresses were close to the maximum allowable stress of 1.81×10^7 N/m² and a negligible amount of displacement with a maximum of 0.24 mm, indicating great structural reliability. The simulations showed consistent motion in each of the five joints.

In contrast with standard SCARA architectures, the present architecture provides real advantages in more confined constrained environments, higher accuracy in conjunction with multi-axis movements and improved flexibility in operations. These outcomes indicate that the manipulator could be applicable in contemporary manufacturing environments to execute horizontal and vertical operations. Generally, the modified SCARA manipulator has demonstrated a practical, lower-cost alternative to flexible automation.

Acknowledgments

We are deeply thankful to everyone who contributed to turning an idea into a tangible application. We extend our sincere gratitude to the Management of Vasavi College of Engineering, Hyderabad, for their support in carrying out this work.

References

[1] Yasunori Yamazaki, "Development and Applications of the SCARA Robot," *Journal of Robotics and Mechatronics*, vol. 26, no. 2, pp. 127-133, 2014. [CrossRef] [Google Scholar] [Publisher Link]

[2] Morteza Shariateesi et al., "Design of an Economical SCARA Robot for Industrial Applications," *2014 Second RSI/ISM International Conference on Robotics and Mechatronics (ICRoM)*, Tehran, Iran, pp. 534-539, 2014. [CrossRef] [Google Scholar] [Publisher Link]

[3] Sonick Suri et al., "SCARA Industrial Automation Robot," *2018 International Conference on Power Energy, Environment and Intelligent Control (PEEIC)*, Greater Noida, India, pp. 173-177, 2018. [CrossRef] [Google Scholar] [Publisher Link]

[4] Yousif Ismail Mohammed, and Safwan Mawlood Hussein, "Modeling and Simulation of Industrial SCARA Robot Arm," *International Journal of Engineering and Advanced Technology (IJEAT)*, vol. 4, no. 4, pp. 220-229, 2015. [Google Scholar] [Publisher Link]

[5] See Han Tay, Wai Heng Choong, and Hou Pin Yoong, "A Review of SCARA Robot Control System," *2022 IEEE International Conference on Artificial Intelligence in Engineering and Technology (IICAIET)*, Kota Kinabalu, Malaysia, pp. 1-6, 2022. [CrossRef] [Google Scholar] [Publisher Link]

[6] Devendra P. Garg, "Adaptive Control of Nonlinear Dynamic SCARA Type of Manipulators," *Robotica*, vol. 9, no. 3, pp. 319-326, 1991. [CrossRef] [Google Scholar] [Publisher Link]

[7] M.C. Lee et al., "Implementation of a New Sliding Mode Control for SCARA Robot," *Proceedings of 1995 American Control Conference - ACC'95*, Seattle, WA, USA, pp. 1387-1391, 1995. [CrossRef] [Google Scholar] [Publisher Link]

[8] Rania Bouzid, Jyotindra Narayan, and Hassène Gritli, "Artificial Neural Networks for the Forward Kinematics of a SCARA Manipulator: A Comparative Study with Two Datasets," *2024 ASU International Conference in Emerging Technologies for Sustainability and Intelligent Systems (ICETSIS)*, Manama, Bahrain, pp. 1792-1797, 2024. [CrossRef] [Google Scholar] [Publisher Link]

[9] Panchanand Jha, and B.B. Biswal, "A Neural Network Approach for Inverse Kinematic of a SCARA Manipulator," *IAES International Journal of Robotics and Automation (IJRA)*, vol. 3, no. 1, pp. 52-61, 2014. [CrossRef] [Google Scholar] [Publisher Link]

[10] R.K. Mittle, and I.J. Nagrath, *Robotics and Control*, 1st ed., Tata McGraw-Hill, 2003. [Google Scholar] [Publisher Link]

[11] See Han Tay, Wai Heng Choong, and Hou Pin Yoong, "A Review of SCARA Robot Control System," *2022 IEEE International Conference on Artificial Intelligence in Engineering and Technology (IICAIET)*, Kota Kinabalu, Malaysia, pp. 1-6, 2022. [CrossRef] [Google Scholar] [Publisher Link]

[12] Wang Ning, "Optimized Design of SCARA Robot Large Arm Based on ABAQUS Topology Optimization," *Mechanical Research & Application*, vol. 36, no. 6, pp. 8-11, 2023. [CrossRef] [Google Scholar] [Publisher Link]

[13] Baohong Liu, Yongyi He, and Zhipeng Kuang, "Design and Analysis of Dual-Arm SCARA Robot Based on Stereo Simulation and 3D Modeling," *2018 IEEE International Conference on Information and Automation (ICIA)*, Wuyishan, China, pp. 1233-1237, 2018. [CrossRef] [Google Scholar] [Publisher Link]

[14] Xingyu Qiu, "Forward Kinematic and Inverse Kinematic Analysis of A 3-DOF RRR Manipulator," *Proceedings of the 2024 International Conference on Mechanics, Electronics Engineering and Automation*, pp. 532-543, 2024. [CrossRef] [Google Scholar] [Publisher Link]

[15] Yuzhen Chen et al., "Error Modeling and Sensitivity Analysis of a Parallel Robot with SCARA(Selective Compliance Assembly Robot Arm) Motions," *Chinese Journal of Mechanical Engineering*, vol. 27, pp. 693-702, 2014. [CrossRef] [Google Scholar] [Publisher Link]

[16] Aamir Khan et al., "Vision Guided Robotic Inspection for Parts in Manufacturing and Remanufacturing Industry," *Journal of Remanufacturing*, vol. 11, pp. 49-70, 2021. [CrossRef] [Google Scholar] [Publisher Link]